A QUADRUPLY SENSED CCD TRANSVERSAL FILTER FOR QUADRATURE PHASING

Carlo Morandi[x] and Hans Wallinga[xx]

ABSTRACT

Wide band quadrature phasing elements have many applications in the fields of instrumentation and communication systems. A well known transformation, providing a pure -90^{o} phase shift of the spectral components of the input signal, is the Hilbert transform. This paper describes the design and performance of a 16-element CCD transversal filter that provides both the delayed Hilbert transform and a delayed copy of the input signal. To achieve this the split-electrode taps are grouped together in four independent sections, simultaneously sensed by separate charge integrating amplifiers. Their output signals are summed in two different combinations which provide the two desired transfer functions.

The main advantage of this method is that both the delayed signal and the quadrature signal are obtained simultaneously from one device, using the same tap electrodes. The principle proposed here may also be applied to the realization of other two channel systems where one of the channels requires weighting factors with even symmetry and the other requires weights of the same magnitude but arranged with an odd symmetry. This may, for example, apply to band separation filters.

INTRODUCTION

Hilbert transformers (broadband 90^{o} phase shifters) are becoming the object of extensive investigations (1, 2, 3) because the advances in the field of digital filtering made their realization practical. Besides the applications in SSB modulation (4) and in speech compression systems (5), recent work (6) considers the Hilbert transformer as a building block to provide "staircase" approximations to arbitrary, time varying filter transfer functions.

CTD transversal filters offer an attractive alternative to purely digital filters, since the required number of multiplications and the subsequent summation are performed without computing time and circuit complexity problems. Realizable filters however introduce a delay in the transformed signal path, consequently it is necessary to add an equal delay in the reference path to implement a quadrature phasing system. An experimental quadrature phasing system, employing an odd number of external tap weights, has been reported by Chowaniec and Hobson (7) but the inaccuracy of the weighting factors, determined by external resistors, did not allow any quantitative measurement.

The quadrature system proposed here consists of a CCD filter with split-electrode taps, grouped together in four independent sections, sensed by separate charge amplifiers.

[x]Istituto di Elettronica, Universita di Bologna, Italy.

[xx]Electrical Engineering Dept., Twente University of Technology, Enschede, The Netherlands.

Their outputs are summed in two combinations, providing the desired filter functions.

In this paper the theoretical arguments for this approach and the first experimental results are discussed.

THEORY OF OPERATION

In digital filtering and in CCD filters with variable weighting factors, every "non-zero" weight requires a complex multiplication circuit. In split-electrode CCD filters with constant weighting factors however there is no difference in cost and complexity between a "zero" and a "non-zero" weight. In consequence a Hilbert transformer (H.T.) design with an odd number of taps, in which about half the number of the weighting factors are equal to zero, has no advantage for the split-electrode system. On the contrary, as shown below, the choice of an even number of taps almost doubles the useful bandwidth of the quadrature system.

To implement the quadrature system, first the weighting factors of the H.T. have to be properly chosen (3) to give a minimal magnitude ripple in a frequency band $f_1 \longmapsto (0.5\ f_c - f_1)$ (f_c = clock frequency; f_1 = lowest useful frequency) symmetrically placed within the band allowed by the Nyquist limit. We choosed a 2N = 16 taps design, optimized (3) for $f_1 = 0.1\ f_c$, for which the theoretical ripple of the modulus of the transfer function $H_H(f)$ (f = signal frequency) is about 2 °/oo, so that an experimental larger module ripple can be unambiguously attributed to errors introduced by the device or by the external circuitry. The weighting factors (h_K, K = 0 → 2 N - 1) for the H.T. are antisymmetrical and apart from a delay factor $\exp(-j\ \pi\ (2N - 1)\ f/f_c)$, they yield a purely imaginary transfer function

$$H_H(f) = j\ G_{odd}(f) = j\left\{2 \sum_{K=0}^{N-1} \left[h_K \sin 2\pi\ (N - K - \tfrac{1}{2})\ f/f_c\right]\right\}$$

Fig. 1 shows the behaviour of G_{odd} with frequency.

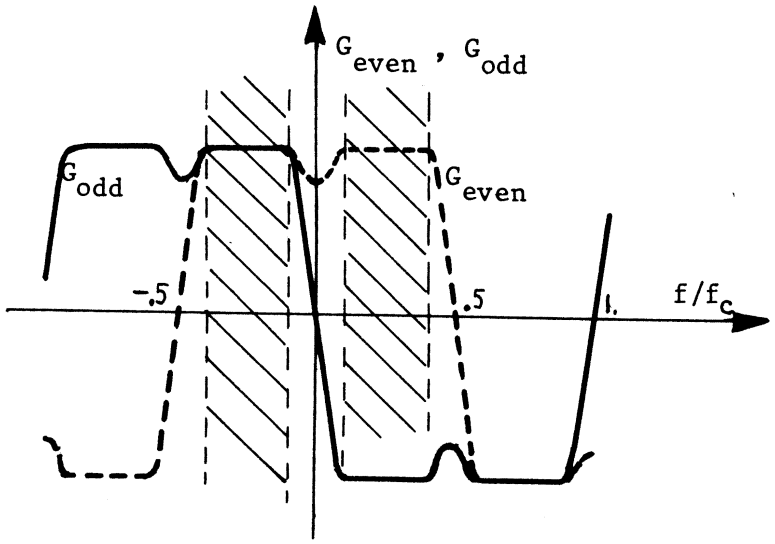

Fig. 1 $G_{odd}(f/f_c)$ and $G_{even}(f/f_c)$. The shaded regions show the useful bandwidth.

A transversal filter with real transfer function $H_D(f) = G_{even}(f) = G_{odd}(f - 0.5\, f_c)$ will within the band $f_1 \longmapsto (0.5\, f_c - f_1)$, act essentially as the delaying filter section (D.S.) required for the quadrature system. It may easily be shown that:

$$G_{even}(f) = 2 \sum_{K=0}^{N-1} \left[(-1)^K h_K \cos 2\pi (N - K - \tfrac{1}{2}) \frac{f}{f_c} \right]$$

$$= 2 \sum_{K=0}^{N-1} \left[h'_K \cos 2\pi (N - K - \tfrac{1}{2}) \frac{f}{f_c} \right]$$

The new weighting factors $h'_K = (-1)^K h_K$ obey the symmetry relation $h'_K = h'_{2N-K-1}$. $G_{even}(f)$ is also represented in fig. 1, where the useful bandwidth of the quadrature system is put in evidence, to clarify the reason why a Hilbert transformer design optimized for a band symmetrically placed in the interval 0 -0.5 f_c is advisable. It should be noticed that if the quadrature system has to operate in a frequency range of P octaves, the bandwidth that should be optimized, normalized to the clock frequency f_c, for an odd number of taps is about twice as large as for an even number of taps. For an even tap number the optimization should extend over the normalized frequency range $f_1/f_c \longmapsto f_1/f_c\, 2^P$, an odd number of taps requires an optimized normalized frequency range of $f_1/f \longmapsto f_1/f_c(2^{PH}+1)$

The actual implementation of the split-electrode filter is schematically shown in fig. 2.

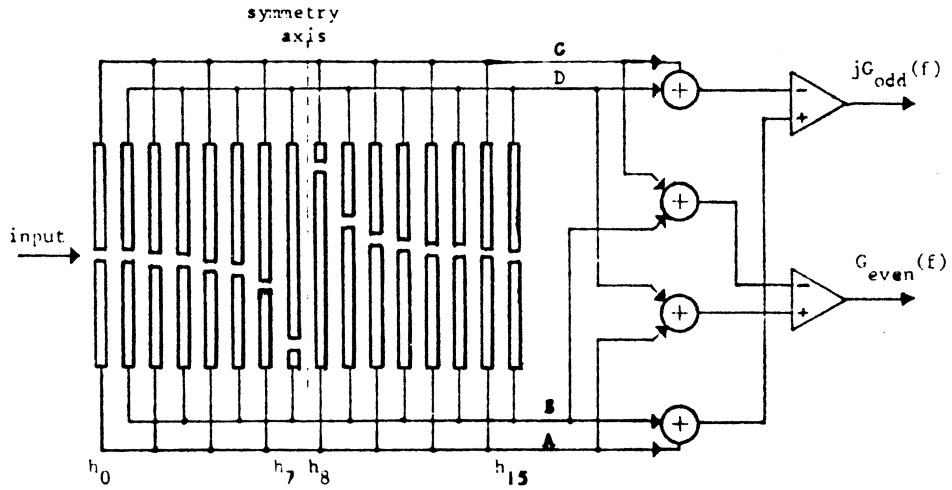

Fig. 2 The quadruply sensed CCD transversal filter for quadrature phasing.

The sensing gates are combined in four groups, A, B, C and D, simultaneously sensed by four separate amplifiers. The H.T. function, requiring antisymmetric weights, is obtained by summing the four outputs as (A + B) - (C + D). The delay-line function (symmetric weights) is obtained as (A + D) - (B + C).

The advantages of this approach are that the tap weights for both filters are determined in one masking step, and that both the delayed signal and the quadrature signal are obtained simultaneously from the same device.

Each element of the sampled output sequence $V_{s,out}(nT)$ is multiplied by a time dependent shape function $g(t - nT)$ which depends on the circuit used to detect the weighted signal charge. The electrical output signal can therefore be described as

$$V_{out}(t) = \sum_{-\infty}^{\infty} V_{s,out}(nT)\, g(t - nT)$$

The Fourier transform of the output signal will then be

$$V_{out}(f) = F\{g(t)\} \cdot DFT\{V_{s,out}(nT)\} \cdot f_c$$

and it is thus clear that the frequency behaviour of $F\{g(t)\}$ will affect the final transfer function of the filter. This has two consequences for our system. First, since it is a broadband system, it is important to operate with a g(t) that does not affect sensibly the transfer function. If this condition is not met, for instance when a sample and hold amplifier is used at the output, which implies a g(t) whose Fourier transform has a modulus rapidly decreasing with frequency, the filter weighting factors should be optimized taking into account the particular shape of g(t). Second, g(t) should be the same for both the D.S. and the H.T. outputs. If for instance the two g's were equal in shape, but one delayed with respect to the other, a phase error proportional to frequency would be introduced.

DEVICE DESCRIPTION

The described functions are implemented in a 16-element transversal CCD filter. It is a p-channel surface CCD with poly-Si storage gates overlapped by Al transfer gates. The technological parameters are summarized in table I.

Table I

	poly Si gates	Al gates
threshold voltage	- 1.6 V	- 3.0 V
oxide thickness	0.125 µm	0.25 µm
gate length	15 µm	10 µm
	channel width	300 µm
	substrate doping N_D	5.10^{14} cm^{-3}

The input signal is applied to the second gate (poly Si), the sampling pulse to the input diode, and the first gate is held a constant DC potential. The filter section consists basically of a 16-element 2-phase CCD driven with a 1-phase clock, to avoid clocking of the sense-gates.

The Al transfer gates, preceding the sense gates are at a DC potential. The sensing poly-Si gates are split in two sections. The difference between the areas of the two sections determines the weighting factor. The channel separation between the two electrode parts is determined by the same channel stop-diffusion which defines the channel width. Thus no alignment errors are introduced. The split gates are grouped together in 4 sections (fig. 2). Each section is on-chip connected to the gate of a source follower MOST, to the source of a reset MOST and to a poly-Si-Al capacitor in parallel with the reset MOST.

Each of the 4 sections is sensed by a separate external charge integrating amplifier, using the on-chip capacitor and reset MOST in the feedback loop (fig. 3).

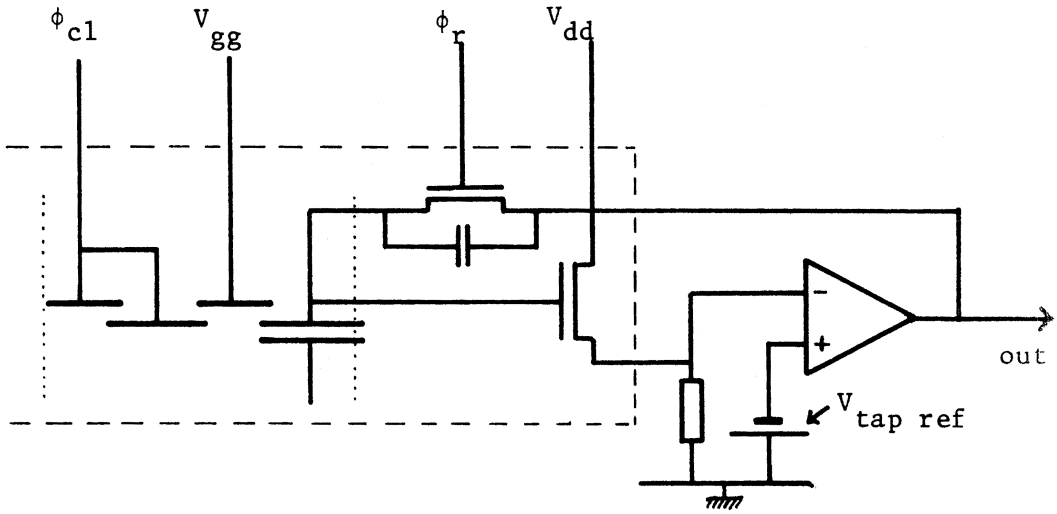

Fig. 3 The charge integrating sense amplifier circuit, schematically drawn for one CCD element and one tap of the split gate The circuitry within the broken line is integrated on the chip.

Integration of the source follower, the reset MOST and the feedback capacitor with the CCD is attractive since sensed gates, which are very sensitive to cross-talk, do not require any external connection.

At the end of the channel the charge is drained by a diffused region and can be sensed by a source follower circuit. A microphotograph of the device is shown in fig.4.

EXPERIMENTAL RESULTS AND ERROR DISCUSSION

In the external circuitry the most important devices are the charge integrating amplifiers and the differential summing amplifiers. For reasons that will be explained below, we employed high slew rate operational amplifiers (120 V/μs).

The impulse response of the system is shown in fig. 5. In fig. 6 the outputs of the H.T. and the D.S. are shown for a sinusoidal input signal. They demonstrate the 90^{o} phase shift between the two sections.

Measurements on the transfer function modulus and distortion measurements were performed with a spectrum analyzer. All the data in this section apply for a clock frequency of 100 kHz.

Second harmonic distortion of both the quadrature and the delayed signal are below - 50 dB. The distortion measurements are performed according to (9). The signal amplitude at the input was 750 mV, corresponding to half of the input dynamic range.

Typical transfer functions are shown in fig. 7. The ripple in the amplitude is for both channels within 1.5%. The slight decrease in amplitude with increasing frequency can be thoroughly explained with the influence of the shape of the output pulse on the transfer function, as discussed in the theory section.

The phase of both filter outputs has been measured with reference to the input signal with a vector lock-in amplifier. The deviation from a 90^{o} phase shift between the H.T. output and the D.S. output is shown in fig. 8. The maximum deviation from a 90^{o} phase shift within the useful bandwidth is 2^{o}. It should be noticed that the design provides a flat amplitude response in the band $0.1\ f_c \longmapsto 0.4\ f_c$, but the 90^{o} phase shift holds theoretically over the complete range $0 \longmapsto 0.5\ f_c$. Fig. 8 shows a correct phase relation in the range $0.05\ f_c \longmapsto 0.45\ f_c$. Near the frequencies 0 and $0.5\ f_c$ the phase relation is, as expected, extremely sensitive to errors.

Experiments have shown that the performance of the external circuitry is of great influence on the phase characteristics, particularly when the clock coupling to the different channel sections is not equal. For the H.T. output (A + B) - (C + D), the coupling of clock transients is fully compensated. However the sections A and D occupy a larger gate area than the sections B and C. Consequently the D.S. output (A + D) - (B + C) is affected by a not fully compensated clock coupling.

If differential amplifiers with moderate slew rates are used, this results in a delay at the output, which depends on the amplitude of the uncompensated part of the clock transients. In the phase relation this causes a deviation from the 90^{o} phase shift, which increases linearly with the signal frequency. In our set-up, this effect could be reduced either by external clock compensation or by using the fast settling differential amplifiers.

It is expected that inclusion of a parallel channel for clock compensation, as described in (8) will completely avoid the problems associated with unequal clock-coupling on the two filter sections, even when low cost differential amplifiers are used.

As mentioned in the device description it is important that the nodes connected to external circuitry see a low impedance to ground. In a first experimental arrangement with external reset transistors and feedback capacitors, a sensible coupling between input and output signal was observed, both directly in the impulse response of the filter and less directly in its frequency response.

Other sources of error arise from the split electrode weighting factors. An accurate positioning of the stopper diffusion islands, defining the tap weights is important. Also variations in the gate length across the channel width and gate oxide variations may influence the tap weight factors in a random way.

The effect of such a random error in the weighting factors on the performance of the quadrature system has been simulated with the Monte Carlo technique (8). Errors in the external circuitry that combines the four output signals are not taken into account. Fig. 9 shows the probability $P_{\Delta\rho}$ that, within the useful bandwidth, the percentual difference $\Delta\rho$ between the magnitudes of the two transfer functions will not exceed the value on the abscissa. Fig. 10 shows in a similar way the probability $P_{\Delta\phi}$ that the deviation $\Delta\phi$ from the 90^{o} phase shift is below the value on the abscissa. The observed discrepancies from the theoretical performance may therefore be attributed to random errors of the order of 1%, but to the opinion of the authors a considerable part of the observed error is still due to the external circuitry.

CONCLUSIONS

This presentation discusses the theoretical and experimental behaviour of a novel realization of a quadrature system, consisting of two transversal filters, combined in one 16-element CCD with split gate semsomg electrodes.

Experimental characteristics show within the useful bandwidth $(0.1 \longmapsto 0.4)\ f_c$ a magnitude flatness of the transfer functions of 1.5% and phase quadrature within 2^{o}.

Sources of errors which could explain the deviation from theoretical performance are input-output coupling, clock transient coupling, random errors in tap weight factors and summation errors in the external circuitry.

In the presented design, input-output coupling has been substantially reduced by integrating a part of the sense circuits. Clock transients in the output signals make high demands upon the external amplifiers. With a careful design of the system, clock transients can almost be avoided. Then it is allowed to use less expensive external circuitry.

Furthermore it is expected that with a larger number of elements, sufficient performance can be achieved over a broader bandwidth. The presented design is also suitable as a building block in more complicated systems. For practical applications the number of taps and the tap weight factors might be optimized according to the special demands.

Finally this system turns out to be a nice tool for investigation of the CCD transversal filters, due to the easily accessable 4 groups, which can be sensed and combined in different ways. The simple shape of the transfer function modulus and the uncomplicated theoretical phase relation facilitate the interpretation of deviations from theoretical behaviour.

ACKNOWLEDGEMENT

The authors like to acknowledge the continuous interest of the members of the Solid-State Electronics Group of the Twente University and are particularly grateful to J. Holleman, who processed the devices and to E.M. Holl, who assisted in building the external circuitry. They wish to thank O.W. Memelink and O. Herrmann for their encouragement and fruitful discussions. C. Morandi also wishes to thank CNR-LAMEL Laboratory for supporting his stage at Twente University.

REFERENCES

1. O. Herrmann; Arch. Elek. Ubertr.,23,(1969),pp. 581-587.

2. B. Gold, A.V. Oppenheim and C.M. Rader; Proc. Symp. Computer Proc. in Communication, (1967), pp. 235-250.

3. L.R. Rabiner and R.W. Schafer; Bell System Techn. J., 53, (1974), pp. 363-390.

4. C.F. Kurth; IEEE Trans. on Circ. and Syst., CAS-23, (1976), pp. 1-17.

5. M.R. Schroeder, J.L. Flanagan and E.H. Lundry; Proc. IEEE, 55, (1967), pp. 396-401.

6. G.D. Cain, A.H. Abed and A. Abu El-Ata; 1975 Florence Conf. on Dig. Sign. Process. Technical Mem. SPG-8.

7. A. Chowaniec and G.S. Hobson; Solid-State Electr., 19, (1976), pp. 201-207.

8. R.D. Baertsch, W.E. Engeler, H.S. Goldberg, C.M. Puckette and J.J. Tiemann; IEEE Trans. El. Dev., ED-23, (1976), pp. 133-141.

9. C.H. Sequin and A.M. Mohsen; IEEE Jnl. of Sol. St. Electr., SC-10, (1975), pp. 81-92.

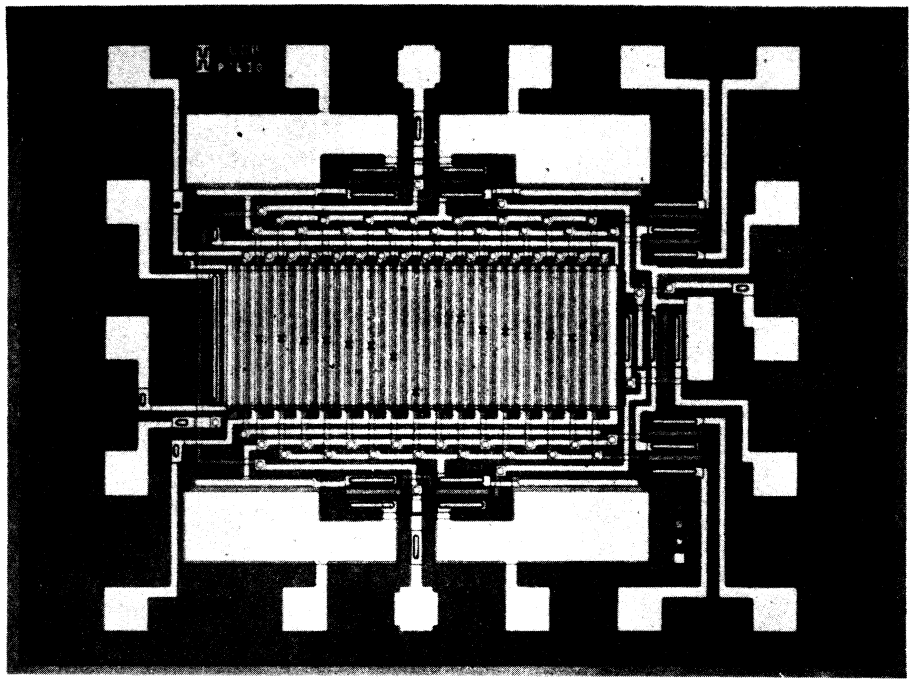

Fig. 4 Microphotograph of the 16-element quadruply sensed CCD transversal filter for quadrature phasing.

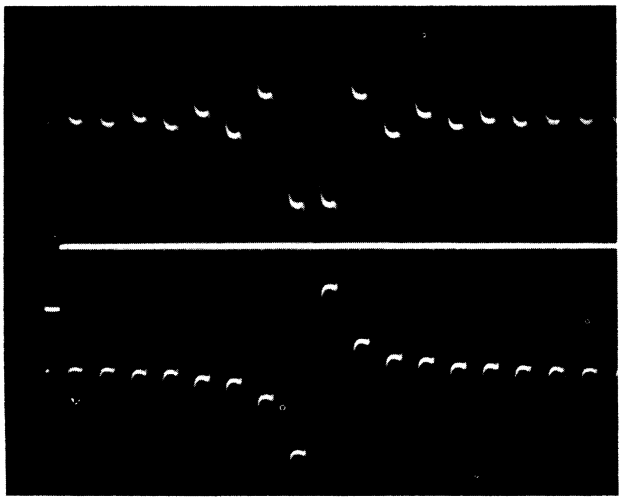

Fig. 5 Impulse response of the quadrature phasing system; upper and lower traces: resp. D.S. and H.T. output, 50 mV/div; middle trace: input pulse 1 V/div; time axis 20 μs/div.

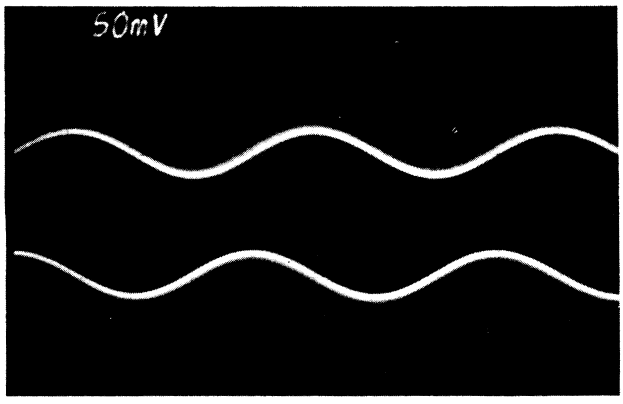

Fig. 6 Output responses of H.T. and D.S. on a sine wave input, demonstrating the 90° phase shift. Vert.: 50 mV/div; hor.: 25 μs/div.

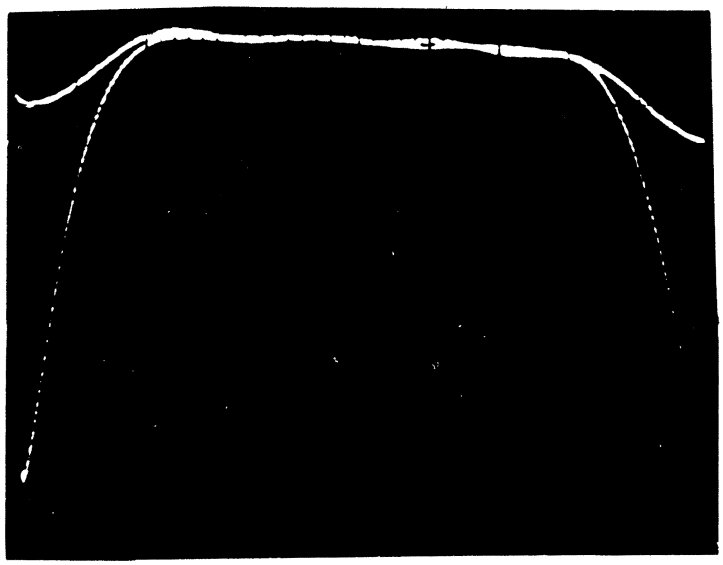

Fig. 7 Transfer function modulus of both the H.T. and the D.S. output. Hor.: frequency, linear scale 0 → 50 kHz. Vert.: amplitude, linear scale.

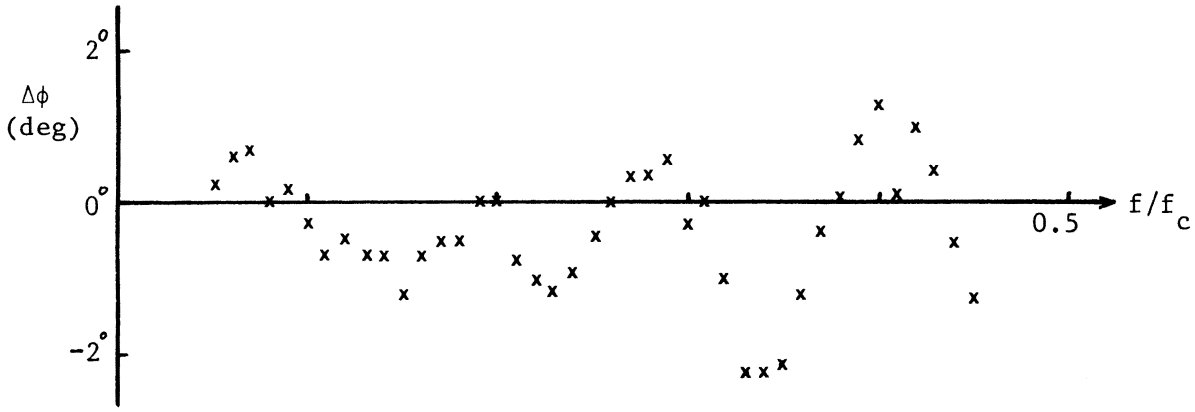

Fig. 8 The experimental deviations from the 90° phase shift between the two filter outputs. Input signal ampl. 100 mV.

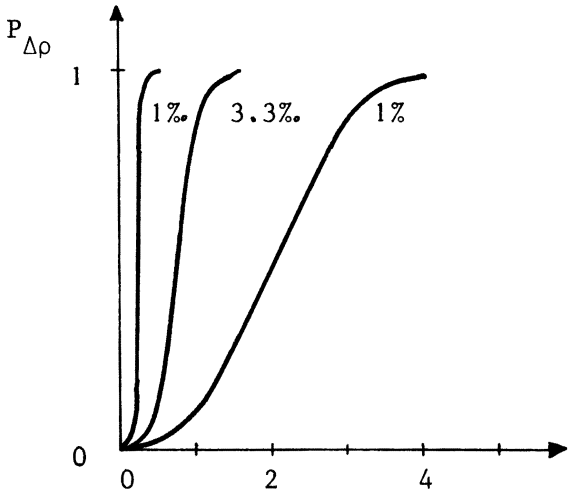

Fig. 9 Magnitude difference (%)

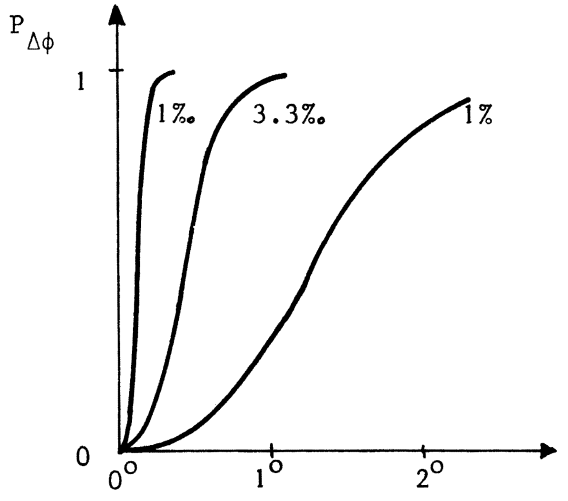

Fig. 10 Phase error (degrees)

Figs. 9 and 10. The probabilities $P_{\Delta\rho}$ and $P_{\Delta\phi}$ that the magnitude differences $\Delta\rho$ and the phase errors $\Delta\phi$ will not exceed the values reported on the abscissas. The curves refer to errors which range with uniform probability within resp. $\pm$ 1.0%, $\pm$ 0.33% and $\pm$ 0.1% of the maximum weighting factor.